Impact of limited statistics on the measured hyperorder cumulants of net-proton distributions in heavy-ion collisions

Lizhu Chen [1,2,*] Ye-Yin Zhao,[3] Yunshan Cheng [4,†] Gang Wang [4] Zhiming Li [2] and Yuanfang Wu [2]

[1]*School of Physics and Optoelectronic Engineering, Nanjing University of Information Science and Technology, Nanjing 210044, China*

[2]*Key Laboratory of Quark and Lepton Physics (MOE) and Institute of Particle Physics, Central China Normal University, Wuhan 430079, China*

[3]*School of Physics and Electronic Engineering, Sichuan University of Science and Engineering (SUSE), Zigong 643000, China*

[4]*Department of Physics and Astronomy, University of California, Los Angeles, California 90095, USA*

(Received 25 January 2024; accepted 16 February 2024; published 18 March 2024)

Hyperorder cumulants C_5/C_1 and C_6/C_2 of net-baryon distributions are anticipated to offer crucial insights into the phase transition from quark-gluon plasma to hadronic matter in heavy-ion collisions. However, the accuracy of C_5 and C_6 is highly contingent on the fine shape of the distribution's tail, the detectable range of which could be essentially truncated by low statistics. In this paper, we use the fast Skellam-based simulations, as well as the ultrarelativistic quantum molecular dynamics model, to assess the impact of limited statistics on the measurements of C_5/C_1 and C_6/C_2 of net-proton distributions at lower energies available at the BNL Relativistic Heavy Ion Collider. Both ratios decrease from the unity baseline as we reduce statistics and could even turn negative without a pertinent physics mechanism. By incorporating statistics akin to experimental data, we can replicate the net-proton C_5/C_1 and C_6/C_2 values comparable to the corresponding measurements for Au + Au collisions at $\sqrt{s_{NN}} = 7.7$, 11.5, and 14.5 GeV. Our findings underscore a caveat to the interpretation of the observed beam energy dependence of hyperorder cumulants.

DOI: 10.1103/PhysRevC.109.034911

I. INTRODUCTION

Cumulants, especially those of higher order, for conserved quantities in relativistic heavy-ion collisions, are crucial observables to probe the phase structure of quantum chromodynamics (QCD) [1]. Conventionally, the cumulants are expressed as

$$C_1 = \langle N \rangle, \tag{1}$$

$$C_2 = \langle (\delta N)^2 \rangle, \tag{2}$$

$$C_3 = \langle (\delta N)^3 \rangle, \tag{3}$$

$$C_4 = \langle (\delta N)^4 \rangle - 3\langle (\delta N)^2 \rangle^2, \tag{4}$$

$$C_5 = \langle (\delta N)^5 \rangle - 10\langle (\delta N)^2 \rangle \langle (\delta N)^3 \rangle, \tag{5}$$

$$C_6 = \langle (\delta N)^6 \rangle + 30\langle (\delta N)^2 \rangle^3 - 15\langle (\delta N)^2 \rangle \langle (\delta N)^4 \rangle - 10\langle (\delta N)^3 \rangle^2, \tag{6}$$

where $\delta N = N - \langle N \rangle$, N is the number of particles in one event, and the average is taken over all events. In practice, cumulant ratios such as C_2/C_1, C_3/C_2, C_4/C_2, C_5/C_1, and C_6/C_2 are employed to mitigate the trivial volume dependence [2]. A Skellam distribution, defined as the difference between two independent Poisson distributions, is typically utilized as a statistical baseline [3,4], which is unity for C_4/C_2, C_5/C_1, and C_6/C_2.

Net-baryon C_5/C_1 and C_6/C_2 are of great interest as lattice QCD calculations [5] show that both of them are negative at low baryon chemical potential (μ_B) near a pseudocritical temperature and become more negative as μ_B increases. Additionally, the QCD-assisted low-energy effective theory and the QCD-based models, such as the Polyakov loop extended quark-meson model and the Nambu-Jona-Lasinio model, also indicate that these two ratios turn negative near the chiral crossover transition [6–10]. In experiments, neutrons are usually undetectable, and the net-proton number (ΔN_p) is measured as a proxy for the net-baryon number [11]. The STAR Collaboration has reported the beam energy and collision centrality dependence of net-proton C_5/C_1 and C_6/C_2 in Au + Au collisions at center-of-mass energies ($\sqrt{s_{NN}}$) from 3 to 200 GeV [12,13]. Except at 3 GeV, the measured C_6/C_2 values for 0–40% centrality collisions display a progressively negative trend with decreasing energy, resembling the aforementioned lattice QCD calculations. Conversely, C_5/C_1 for 0–40% centrality collisions from 7.7 to 200 GeV exhibits a weak beam energy dependence and fluctuates about zero.

Before connecting the measured C_5/C_1 and C_6/C_2 to lattice QCD calculations, however, it is vital to eliminate contributions unrelated to the phase transition. For instance, the hadron resonance gas model can also produce negative net-baryon C_6/C_2 values at $\sqrt{s_{NN}} \lesssim 40$ GeV by integrating global baryon-number conservation [14]. Similar negative behaviors in C_6/C_2 are also noted in the subensemble acceptance method [15–17] and hydrodynamics calculations [18], encompassing global conservation, system nonuniformity, and momentum

*chenlz@nuist.edu.cn

†yunshancheng@physics.ucla.edu

space acceptance. Moreover, it is imperative to consider other mechanisms, including initial volume fluctuations [19–21], as well as distinctions between net-proton and net-baryon cumulants [11,22,23].

Beyond physics mechanisms, insufficient statistics can also affect the hyperorder cumulant measurements [24–27]. Cumulants reflect the shape of the distribution. For example, skewness ($C_3/C_2^{3/2}$) reveals left-right asymmetry, and kurtosis (C_4/C_2^2) quantifies the peakedness of the distribution or the fatness of the tail. Hyperskewness (C_5/C_1) and hyperkurtosis (C_6/C_2) are also indicators of left-right asymmetry and tail fatness, respectively. These measures, with a heightened emphasis on values far from the mean, exhibit particular sensitivity to the fine details of the distribution's tail. When the data analyses involve low statistics, the distribution's tail may not be fully explored and can be essentially truncated. The resultant hyperorder cumulants are thus distorted. In this scenario, the observed C_5/C_1 and C_6/C_2 can be negative even with statistical Skellam-based simulations. Additionally, to suppress initial volume fluctuations, data analyses commonly apply the centrality bin width correction (CBWC) [28–30], by conducting statistics within each multiplicity bin before aggregating the results for a finite centrality interval. This exacerbates the impact of low statistics on the measured hyperorder cumulants.

In Sec. II, we use a Skellam distribution to illustrate how the sampling of the distribution's tail, or rather the lack thereof, influences the measured C_5/C_1 and C_6/C_2. In Sec. III, we corroborate the impact of limited statistics, especially the CBWC-induced effect, on both hyperorder cumulants using a more realistic model, ultrarelativistic quantum molecular dynamics (UrQMD) [31,32]. In Sec. IV, we present comprehensive Skellam-based Monte Carlo simulations with statistics akin to experimental data at lower energies available at the BNL Relativistic Heavy Ion Collider (RHIC) and compare the outcomes with the data. Finally, we provide a summary in Sec. V.

II. STATISTICAL SKELLAM SIMULATIONS

We start the investigation of low-statistics effects with the statistical baseline using a Skellam distribution,

$$f(k,\mu_1,\mu_2) = e^{-(\mu_1+\mu_2)}\left(\frac{\mu_1}{\mu_2}\right)^{\frac{k}{2}} I_{|k|}(2\sqrt{\mu_1\mu_2}), \qquad (7)$$

where $I_{|k|}(z)$ is the modified Bessel function of the first kind. The input parameters, $\mu_1 = 31.217$ and $\mu_2 = 0.96272$, match the STAR measurements of $\langle N_p\rangle$ and $\langle N_{\bar{p}}\rangle$, respectively, in 0–5% most central Au + Au collisions at $\sqrt{s_{NN}} = 11.5$ GeV [28], in which the number of analyzed events is around 10^6.

Figure 1 displays the normalized ΔN_p distribution according to Eq. (7). With total statistics of 10^6 events, detecting an event with a probability below 10^{-7} to 10^{-6} is rather improbable. The region with $\Delta N_p \geqslant 58$ has a cumulative probability of roughly 6.35×10^{-6}, suggesting an expectation of only 6 or 7 events occurring within this tail. This tail has a negligible impact on lower-order cumulants, but not on hyperorder ones. For instance, its contribution to C_1 (≈ 30.2543) is only 0.0004, constituting a relative 0.0013%. However, an extra event with $\Delta N_p = 60$ will already add 24.3 and 729 to the first terms of C_5 ($= C_1 \approx 30.2543$) and C_6 ($\approx$32.1792), respectively, as defined in Eqs. (5) and (6). Let alone other terms of C_5 and C_6. In the left tail, events with ΔN_p between -2 and 6 have probabilities ranging from 10^{-12} to 10^{-7}, and their contributions to C_5 and C_6 are minimal compared with those in the right tail. For the demonstration purpose, we focus on events with ΔN_p in the right tail with probabilities below 10^{-6}.

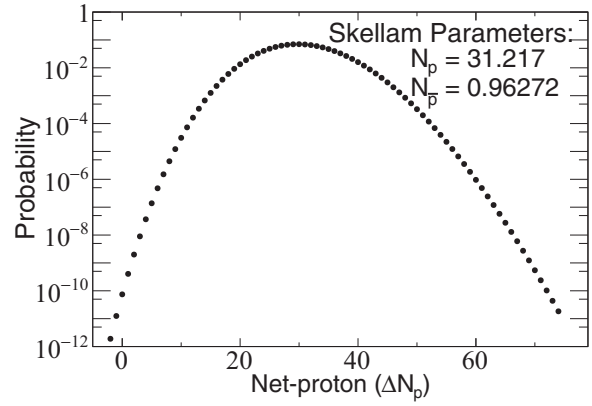

FIG. 1. Probability of the net-proton number (ΔN_p) based on the Skellam distribution in Eq. (7).

Figures 2(a) and 2(b) show the truncation effects on C_5/C_1 and C_6/C_2, respectively, which are calculated by excluding events with ΔN_p exceeding a certain upper bound, $\Delta N_p^{\rm up}$. When $\Delta N_p^{\rm up}$ is around 70, both C_5/C_1 and C_6/C_2 adhere closely to the unity baseline, indicated by red dashed lines. As we reduce $\Delta N_p^{\rm up}$, both hyperorder cumulants decrease and could even turn negative with severe truncation. With $\Delta N_p^{\rm up} = 60$, the resulting C_6/C_2 surpasses in magnitude the aforementioned physics mechanisms unrelated to the phase transition.

In experiments, events in the right tail might be missing from analysis due to detector limitations or event selection. For example, a single good event occurring once in a 10^6

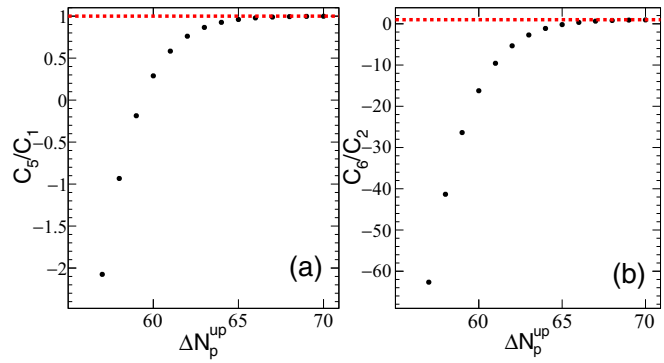

FIG. 2. (a) C_5/C_1 and (b) C_6/C_2 calculated with artificial truncation on the distribution in Fig. 1, excluding events with ΔN_p exceeding the upper bound $\Delta N_p^{\rm up}$. The red dashed lines at unity serve as the expected baselines.

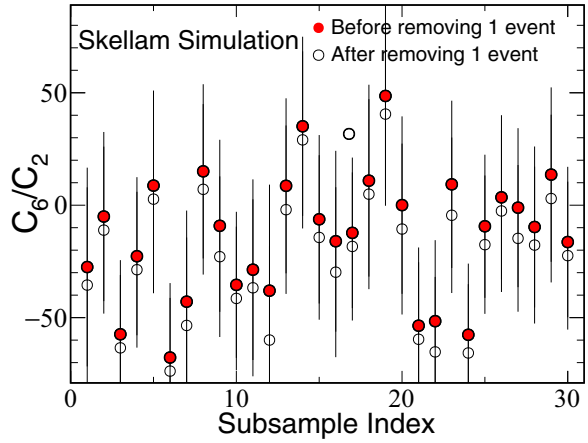

FIG. 3. Skellam-based Monte Carlo simulations of C_6/C_2 (a) before and (b) after randomly rejecting one event with $\Delta N_p > 58$ from each subsample of 10^6 events.

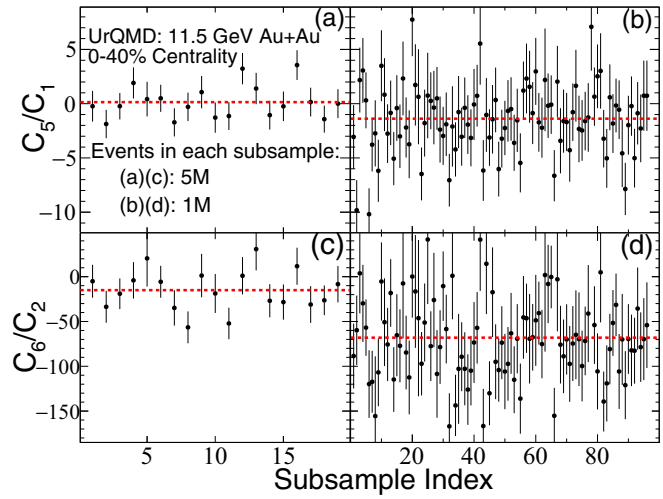

FIG. 4. UrQMD calculations of net-proton C_5/C_1 (upper panels) and C_6/C_2 (lower panels) in 0–40% Au + Au collisions at $\sqrt{s_{NN}} = 11.5$ GeV. The entire sample of 9.6×10^7 events is divided into subsamples of 5×10^6 (left panels) or 10^6 (right panels) events. The red dashed lines represent the ensemble averages over all subsamples.

instances might be erroneously excluded by the quality assurance procedure. To examine this effect, we randomly generate 30 independent subsamples, each with 10^6 events following the same Skellam distribution, as depicted in Fig. 1. From each subsample, we randomly reject one event with $\Delta N_p > 58$. Figure 3 presents the C_6/C_2 values before (solid circles) and after (open circles) removing one event. The latter values are consistently lower than the former. This effect is expected to be more pronounced for even higher-order cumulants, such as C_8, necessitating careful treatments in data analyses.

III. UrQMD SIMULATIONS FOR AU + AU COLLISIONS AT $\sqrt{s_{NN}} = 11.5$ GeV

The CBWC method in data analyses divides events from each centrality interval into finer multiplicity bins, leading to an essential reduction in the effective statistics and thus exacerbating the low-statistics effect on the measurements of hyperorder cumulants. We examine the CBWC-induced low-statistics effect on net-proton C_5/C_1 and C_6/C_2 using the UrQMD model (version 3.4) [31,32]. In this study, multiplicity is quantified with the third category of reference multiplicity (RefMult3), the number of charged pions and kaons within the pseudorapidity range of $|\eta| < 1$ in each event, to avoid autocorrelations. RefMult3 corresponds to the same quantity as that adopted in the STAR experiment [33]. For a given centrality, cumulants (C_1, C_2, C_5, and C_6) are initially computed within each RefMult3 bin and then averaged over all RefMult3 bins, with the event number serving as a weight. The kinematic regions for (anti)protons are $0.4 < p_T < 2\,\text{GeV}/c$ and $|y| < 0.5$. The statistical errors are estimated using the bootstrap method [34,35].

We have generated 9.6×10^7 UrQMD events for 0–40% Au + Au collisions at $\sqrt{s_{NN}} = 11.5$ GeV, matching the same statistics as experimental data [13]. The complete sample is randomly divided into 19 or 96 subsamples, each containing 5×10^6 (5M) or 10^6 (1M) events. Figures 4(a) and 4(b) depict the net-proton C_5/C_1 values from the 5M and 1M subsamples, respectively, and Figs. 4(c) and 4(d) delineate the corresponding results for C_6/C_2. The red dashed lines represent the ensemble averages in each scenario, denoted by $\langle C_5/C_1\rangle_{5\text{M}}$, $\langle C_5/C_1\rangle_{1\text{M}}$, $\langle C_6/C_2\rangle_{5\text{M}}$, and $\langle C_6/C_2\rangle_{1\text{M}}$, respectively. Both $\langle C_6/C_2\rangle_{5\text{M}}$ and $\langle C_6/C_2\rangle_{1\text{M}}$ are negative in UrQMD simulations, without invoking any phase transition. Moreover, $\langle C_6/C_2\rangle_{1\text{M}}$ is significantly lower than $\langle C_6/C_2\rangle_{5\text{M}}$, corroborating the CBWC-induced low-statistics effect. The CBWC-related effect on C_5/C_1 is also noteworthy, albeit to a lesser extent. It is reasonable to assume that higher-order cumulants are more vulnerable to the low-statistics effect.

IV. STATISTICS DEPENDENCE OF C_5/C_1 AND C_6/C_2 AT LOWER ENERGIES AVAILABLE AT RHIC

As UrQMD calculations are computationally intensive, we instead perform fast Skellam-based Monte Carlo simulations to comprehensively study the statistics dependence of net-proton C_5/C_1 and C_6/C_2. We generate numerous subsamples, each comprising 5×10^6 (5M) or 10^6 (1M) events. In each event, RefMult3 follows the same distribution as from UrQMD, and N_p and $N_{\bar{p}}$ obey Poisson distributions, with $\langle N_p\rangle$ and $\langle N_{\bar{p}}\rangle$, respectively, derived from the corresponding RefMult3 bin in UrQMD. In the calculation of net-proton hyperorder cumulants, the CBWC approach is applied based on RefMult3.

Figure 5 illustrates the Skellam-based Monte Carlo simulations of net-proton C_6/C_2 from 50 subsamples for both (a) 5M and (b) 1M scenarios in 0–40% Au + Au collisions at 11.5 GeV. The red dashed lines represent $\langle C_6/C_2\rangle_{5\text{M}}$ and $\langle C_6/C_2\rangle_{1\text{M}}$, each averaged over 1000 subsamples. Both $\langle C_6/C_2\rangle_{5\text{M}}$ and $\langle C_6/C_2\rangle_{1\text{M}}$ are significantly below zero, while $\langle C_6/C_2\rangle_{5\text{M}}$ is higher than $\langle C_6/C_2\rangle_{1\text{M}}$. For comparison, we also show the UrQMD results of $\langle C_6/C_2\rangle \pm 2\sigma$ extracted from Figs. 4(a) and 4(b), indicated with blue shaded bands. Despite differences in event-generating mechanisms, the

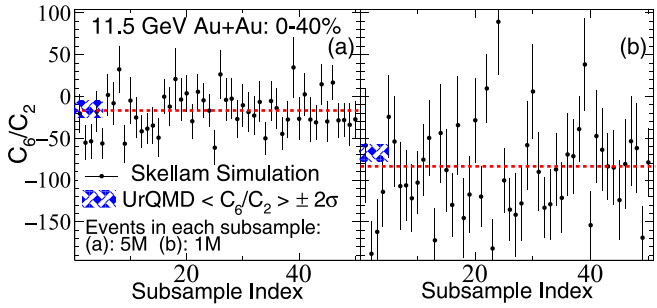

FIG. 5. Skellam-based simulations of net-proton C_6/C_2 for 0–40% Au + Au collisions at $\sqrt{s_{NN}} = 11.5$ GeV using subsamples of (a) 5×10^6 or (b) 10^6 events. The RefMult3 distribution and $\langle N_p \rangle$ and $\langle N_{\bar{p}} \rangle$ for each RefMult3 are taken from the UrQMD model. The red dashed lines represent the ensemble averages over 1000 subsamples. The blue shaded bands denote the UrQMD calculations of $\langle C_6/C_2 \rangle \pm 2\sigma$ extracted from Figs. 4(a) and 4(b).

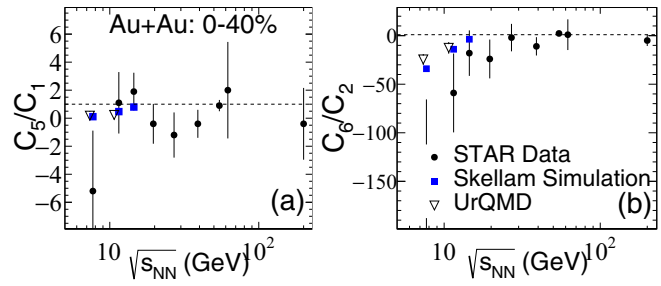

FIG. 7. Skellam-based simulations of the beam energy dependence of net-proton (a) $\langle C_5/C_1 \rangle$ and (b) $\langle C_6/C_2 \rangle$ in 0–40% Au + Au collisions. For comparison, we also show the STAR measurements [12,13] that have the same statistics as the simulations at the overlapping energies. The UrQMD calculations for $\sqrt{s_{NN}} = 7.7$ and 11.5 GeV are slightly offset horizontally to improve clarity. The dashed lines at unity serve as the statistical baselines.

net-proton $\langle C_6/C_2 \rangle$ results exhibit remarkable similarities between UrQMD and Skellam-based simulations, both of which have the same statistics and the same parametrization for RefMult3, $\langle N_p \rangle$, and $\langle N_{\bar{p}} \rangle$. This implies that the C_6/C_2 behavior in UrQMD is dominated by inadequate statistics. In other words, the details in the particle production mechanism cannot be properly revealed by net-proton C_6/C_2 given the currently available statistics.

As the Skellam-based simulation captures the essence of the low-statistics effect on hyperorder cumulant measurements, we employ it to explore the statistics dependence of net-proton C_5/C_1 and C_6/C_2 for 0–40% Au + Au collisions at $\sqrt{s_{NN}} = 7.7$, 11.5, and 14.5 GeV. The C_5/C_1 and C_6/C_2 results are presented in Figs. 6(a)–6(c) and Figs. 6(d)–6(f), respectively. $N_{\rm Evt}$ denotes the number of events in each subsample, and $\langle C_5/C_1 \rangle$ and $\langle C_6/C_2 \rangle$ are computed by averaging

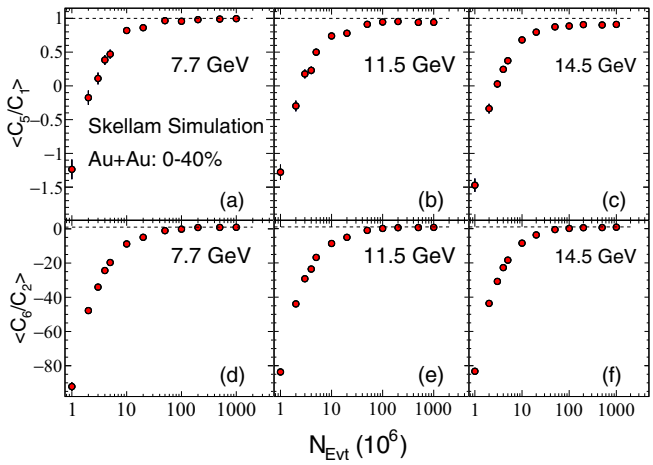

FIG. 6. Statistics dependence of net-proton $\langle C_5/C_1 \rangle$ (upper panels) and $\langle C_6/C_2 \rangle$ (lower panels) in 0–40% Au + Au collisions at $\sqrt{s_{NN}} = 7.7$, 11.5, and 14.5 GeV from Skellam-based Monte Carlo simulations. $N_{\rm Evt}$ denotes the number of events in each subsample. $\langle C_5/C_1 \rangle$ and $\langle C_6/C_2 \rangle$ are computed by averaging over 1000 subsamples. The dashed lines at unity serve as the expected baselines.

over 1000 subsamples. At all energies, $\langle C_6/C_2 \rangle$ increases with the growth of statistics as expected, and analyses with $N_{\rm Evt} < 2 \times 10^7$ render significantly negative $\langle C_6/C_2 \rangle$ values. For the same statistics, the $\langle C_6/C_2 \rangle$ values at different beam energies are close to each other because the input parameters from UrQMD are akin among these energies. $\langle C_6/C_2 \rangle$ approaches zero at $N_{\rm Evt} = 10^8$ and then turns positive but remains below unity at $N_{\rm Evt} = 2 \times 10^8$. This can be attributed to the CBWC procedure, which divides events from each centrality interval into finer RefMult3 bins and reduces the effective statistics in the analysis. Compared with $\langle C_6/C_2 \rangle$, $\langle C_5/C_1 \rangle$ deviates from unity to a lesser extent. At all three beam energies, the $\langle C_5/C_1 \rangle$ values are negative at $N_{\rm Evt} < 3 \times 10^6$ and approach unity at $N_{\rm Evt} > 5 \times 10^7$.

The numbers of events involved in the measurements of net-proton hyperorder cumulants during the RHIC Beam Energy Scan phase I (BES-I) are approximately 3×10^6, 6.6×10^6, and 2×10^7 in 0–40% Au + Au collisions at $\sqrt{s_{NN}} = 7.7$, 11.5, and 14.5 GeV, respectively [13]. Based on the discussions related to Fig. 6, it is evident that these datasets are insufficient to yield reliable measurements for C_5/C_1 and C_6/C_2. Figure 7 shows the beam energy dependence of net-proton (a) $\langle C_5/C_1 \rangle$ and (b) $\langle C_6/C_2 \rangle$ in 0–40% Au + Au collisions from the Skellam-based simulations (blue solid squares). The results are averaged over 1000 subsamples, each having the same statistics as the experimental data at the corresponding energy. The UrQMD calculations (black open triangles) are plotted for 0–40% Au + Au at 7.7(11.5) GeV, and the results are averaged over 35(14) subsamples, each containing 3×10^6 (6.6×10^6) events. The STAR BES-I data (black solid circles) [13] are also presented for comparison, with the statistical and systematic uncertainties combined in quadrature. The C_5/C_1 values from the Skellam-based simulations and UrQMD calculations are predominantly influenced by the low-statistics effect, ranging between 0 and 1 and aligning with the data within the associated uncertainties at all overlapping energies. The C_6/C_2 values from both the Skellam-based simulations and the UrQMD calculations exhibit an ascending trend with beam energy and are

quantitatively consistent with experimental data at all collision energies under study.

V. SUMMARY

Net-proton hyperorder cumulants potentially convey essential information on the phase transition in heavy-ion collisions, but the experimental measurements could be significantly affected by low statistics. We have conducted statistical Skellam simulations to illustrate that insufficient statistics can limit the detectable range of the net-proton (ΔN_p) distribution. Consequently, the derived values of C_5/C_1 and C_6/C_2 decrease from the unity baseline and could even turn negative without any discernible underlying physics. In reality, even if the ΔN_p distribution is not severely truncated, a portion of the distribution's tail might be overlooked due to detector inefficiency or event selection. Accordingly, we have further attempted to exclude one event with $\Delta N_p > 58$ from each subsample of 10^6 events, resulting in significantly lower C_6/C_2 values than the original ones.

In practice, to suppress initial volume fluctuations, the centrality bin width correction (CBWC) necessitates statistical analyses within each multiplicity bin instead of a finite centrality interval, further amplifying the impact of low statistics. We have demonstrated the CBWC-related effect on net-proton C_5/C_1 and C_6/C_2 using UrQMD calculations for the 0–40% centrality range in Au + Au collisions at $\sqrt{s_{NN}} = 11.5$ GeV. The corresponding influence on C_6/C_2 is notably stronger than that on C_5/C_1. The similarity between the results from UrQMD calculations and Skellam-based Monte Carlo simulations suggests that the hyperorder cumulants measured with the statistics involved in this analysis are dominated by the low-statistics effect.

We have further performed fast Skellam-based simulations with RHIC BES-I statistics for 0–40% Au + Au collisions at $\sqrt{s_{NN}} = 7.7$, 11.5, and 14.5 GeV. The resultant net-proton C_5/C_1 spans from zero to unity, whereas the C_6/C_2 values are significantly negative. Both C_5/C_1 and C_6/C_2 are consistent with their corresponding experimental results within the uncertainties. Specifically, the C_6/C_2 values in the simulations distinctly exhibit a decreasing trend as the collision energy decreases from $\sqrt{s_{NN}} = 14.5$ to 7.7 GeV. The concurrence between net-proton hyperorder cumulants from Monte Carlo simulations and real data, both in magnitudes and trends, raises a cautionary note in the interpretation of the observed beam energy dependence at RHIC. It is reasonable to speculate that even higher-order cumulants, such as C_8, will be more susceptible to the low-statistics effect.

The number of collision events collected at RHIC BES-II is typically 10–20 times higher than that at BES-I for each beam energy, and hence the low-statistics effect will be significantly reduced. According to the study presented in this paper, we anticipate that future measurements of both C_5/C_1 and C_6/C_2 from BES-II will show a notable increase compared with the current data. To devise a method for mitigating the impact of limited statistics on the measured hyperorder cumulants, additional theoretical efforts are warranted to develop a realistic event generator that incorporates the physics of the phase transition, along with other mechanisms such as baryon conservation and proton-antiproton correlations.

ACKNOWLEDGMENTS

This work is supported by the National Key Research and Development Program of China (Grant No. 2022YFA1604900), the National Natural Science Foundation of China (Grant No. 12275102), and the Open Fund of Key Laboratory of the Ministry of Education for the Central China Normal Universities (Grant No. QLPL2021P01). Y.C. and G.W. are supported by the U.S. Department of Energy under Grant No. DE-FG02-88ER40424 and by the National Natural Science Foundation of China under Contract No. 1835002. We also acknowledge the High Performance Computing Center of Nanjing University of Information Science and Technology for its support of this work.

[1] A. Bzdak *et al.*, Phys. Rep. **853**, 1 (2020).
[2] M. Cheng *et al.*, Phys. Rev. D **79**, 074505 (2009).
[3] P. Braun-Munzinger, B. Friman, F. Karsch, K. Redlich, and V. Skokov, Phys. Rev. C **84**, 064911 (2011).
[4] X. Pan, F. Zhang, Z. Li, L. Chen, M. Xu, and Y. Wu, Phys. Rev. C **89**, 014904 (2014).
[5] A. Bazavov, D. Bollweg, H. T. Ding, P. Enns, J. Goswami, P. Hegde, O. Kaczmarek, F. Karsch, R. Larsen, S. Mukherjee, H. Ohno, P. Petreczky, C. Schmidt, S. Sharma, and P. Steinbrecher (HotQCD Collaboration), Phys. Rev. D **101**, 074502 (2020).
[6] K. Morita, B. Friman, K. Redlich, and V. Skokov, Phys. Rev. C **88**, 034903 (2013).
[7] V. Skokov, B. Friman, and K. Redlich, Phys. Lett. B **708**, 179 (2012).
[8] B. Friman *et al.*, Eur. Phys. J. C **71**, 1694 (2011).
[9] W. J. Fu, X. Luo, J. M. Pawlowski, F. Rennecke, R. Wen, and S. Yin, Phys. Rev. D **104**, 094047 (2021).
[10] W.-J. Fu *et al.*, arXiv:2308.15508.
[11] M. Kitazawa and M. Asakawa, Phys. Rev. C **86**, 024904 (2012); **86**, 069902(E) (2012).
[12] M. S. Abdallah *et al.* (STAR Collaboration), Phys. Rev. Lett. **127**, 262301 (2021).
[13] B. E. Aboona *et al.* (STAR Collaboration), Phys. Rev. Lett. **130**, 082301 (2023).
[14] P. Braun-Munzinger *et al.*, Nucl. Phys. A **1008**, 122141 (2021).
[15] V. Vovchenko *et al.*, Phys. Lett. B **811**, 135868 (2020).
[16] V. Vovchenko, R. V. Poberezhnyuk, and V. Koch, J. High Energy Phys. 10 (2020) 089.
[17] V. Vovchenko, Phys. Rev. C **105**, 014903 (2022).
[18] V. Vovchenko, V. Koch, and C. Shen, Phys. Rev. C **105**, 014904 (2022).
[19] M. I. Gorenstein and M. Gaździcki, Phys. Rev. C **84**, 014904 (2011).
[20] V. Skokov, B. Friman, and K. Redlich, Phys. Rev. C **88**, 034911 (2013).

[21] P. Braun-Munzinger, A. Rustamov, and J. Stachel, Nucl. Phys. A **960**, 114 (2017).
[22] M. Kitazawa and M. Asakawa, Phys. Rev. C **85**, 021901(R) (2012).
[23] V. Vovchenko and V. Koch, Phys. Rev. C **103**, 044903 (2021).
[24] L.-Z. Chen *et al.*, Chin. Phys. C **45**, 104103 (2021).
[25] L.-Z. Chen, Z.-M. Li, and Y.-F. Wu, J. Phys. G: Nucl. Part. Phys. **41**, 105107 (2014).
[26] L.-Z. Chen *et al.*, J. Phys. G: Nucl. Part. Phys. **42**, 065103 (2015).
[27] L.-Z. Chen *et al.*, Nucl. Phys. A **957**, 60 (2017).
[28] M. S. Abdallah *et al.* (STAR Collaboration), Phys. Rev. C **104**, 024902 (2021).
[29] X. Luo (STAR Collaboration), J. Phys.: Conf. Ser. **316**, 012003 (2011).
[30] X. Luo and N. Xu, Nucl. Sci. Tech. **28**, 112 (2017).
[31] S. A. Bass *et al.*, Prog. Part. Nucl. Phys. **41**, 255 (1998).
[32] M. Bleicher *et al.*, J. Phys. G: Nucl. Part. Phys. **25**, 1859 (1999).
[33] L. Adamczyk *et al.* (STAR Collaboration), Phys. Rev. C **96**, 044904 (2017).
[34] B. Efron, Ann. Stat. **7**, 1 (1979).
[35] A. Pandav, D. Mallick, and B. Mohanty, Nucl. Phys. A **991**, 121608 (2019).